Complex High Frequency Properties of Ceramic-Polymer Nanocomposites: Comparison of Fluoro-Polymers and Acrylic-Based Compounds

Dorothée Vinga Szabó, Iris Lamparth, Dieter Vollath*

Forschungszentrum Karlsruhe GmbH, Institut für Materialforschung III, D-76021 Karlsruhe, P.O. Box 3640, Germany

Summary: Coated nanoparticles are used to produce ceramic-polymer nanocomposites with interesting physical properties. The ceramic cores of the particles are produced in a microwave plasma. The monomers of interest are evaporated and inserted directly after the plasma reaction zone. Acrylic-based monomers, fluorinated monomers and $C_{20}F_{42}$ are used for the polymer coating. The ceramic-polymer nanocomposites generally contain 50 to 70 Vol-% of polymer. The complex high frequency permittivity, $\varepsilon_r = \varepsilon' - j\varepsilon''$, is determined with a vector network analyser in the frequency range from 10 MHz to 8 GHz. The ceramic/polymer nanocomposite shows an increased permittivity compared to that of the pure polymer. Slight frequency dependency is observed. The permittivity can be adjusted by the ceramic/polymer ratios.

Introduction

In the recent years a versatile synthesis method based on the microwave plasma process for the production of polymer coated nanoparticles[1,2,3] has been developed. These polymer-coated nanoparticles type can be compacted easily to nanocomposites. This results in very homogeneous consolidated parts. In such a material different physical and/or chemical properties of the core and the coating may be combined to modify the properties leading to a new material. Superparamagnetism[4] for example, is a property of isolated, non interacting particles with particle sizes below approximately 15 nm that can be transferred into a consolidated worked piece by using polymer coated ferrite nanoparticles as starting material.[5] In this case, the polymer reduces the interaction between the ferrite cores and in addition, acts as binder in the composite material.

More general, in this paper we ask: How are the dielectric properties in nanocomposites modified by combining frequency independent properties of a polymer with frequency dependent ones of ceramics? To find an answer for this question, in this study the complex frequency permittivity $\varepsilon_r = \varepsilon' - j\varepsilon''$, of different Al_2O_3/polymer nanocomposites is measured as a function of the frequency.

 CCC 1022-1360/00/$ 17.50+.50/0

Experimental

Nano-Al_2O_3 nanoparticles (n-Al_2O_3) were produced in a microwave plasma burning in a quartz glass tube passing a microwave cavity. The precursor, $AlCl_3$, is evaporated and introduced with Ar as carrier gas and O_2 as reaction gas in front of the reaction zone. Leaving the plasma zone, nanoparticles formed in the plasma carry electrical charges of the same sign. Therefore, they repel each other. This fact enables coating with a polymer directly after the plasma zone. n-Al_2O_3 produced with the microwave plasma process exhibits particle sizes below 8 nm and therefore, it is amorphous.[6]

Two sets of samples with different ceramic/polymer ratios and different material combinations were prepared.

1. n-Al_2O_3 cores coated with 50 +/- 5vol % polymer derived from one of the following monomers: $C_{20}F_{42}$, $H_2C{=}CH\text{-}COOCH_2CF_2CF_2CF_3$, $H_2C{=}C(CH_3)\text{-}COOCH_3$, or $H_2C{=}C(CH_3)\text{-}COOCH_2CH_2NCO$.
2. n-Al_2O_3 cores coated with 70 +/- 5 Vol-% polymer derived from one of the following monomers: $F_3C\text{-}(CF_2)_{10}COOCH_3$, $H_2C{=}CH\text{-}COO\text{-}(CH_2)_2(CF_2)_9CF_3$, or $F_3C\text{-}(CF_2)_9CH_2CH_2I$.

Details of the sample compositions are summarised in Table 1. The polymer content of the materials was measured gravimetrically. The true density of the material was determined using a Helium-Pycnometer. The open porosity of the samples was derived from the true and the geometric density of compacted samples.

The complex permittivity, $\varepsilon_r = \varepsilon' - j\varepsilon''$, was determined with a vector network analyser (Rohde & Schwarz, ZVC) in the frequency range from 10 MHz to 8 GHz, using the coaxial-line-S-parameter method.[7,8] For sample preparation, the nanopowders were compacted with 200 N/mm^2 to rings of diameter d_i = 1,6 mm and d_a = 3,4 mm, respectively, fitting exactly into a 50 Ω PC 3.5 beadless air line. The sample length varied from 3,0 to 4,2 mm. Correction for phase shift was necessary, since the length of the specimen did not correspond to the one of the sample holder.[9] For the specimen holder in use, the algorithm for data evaluation looses precision at frequencies around 4 GHz.

Results

For a better understanding of this type of materials, Figure 1a and b exhibit as an example the transmission electron micrographs of two different γ-Fe_2O_3/polymer nanocomposites.[2,3] This material was selected for demonstration of the morphology,

because it gives significant contrast in the electron microscope, compared to the poor contrast of Al_2O_3/polymer nanocomposites. The dark regions are the γ-Fe_2O_3 cores, with approximately 5 to 6 nm in diameter. The bright and grey areas around the cores reflect the polymer coating.

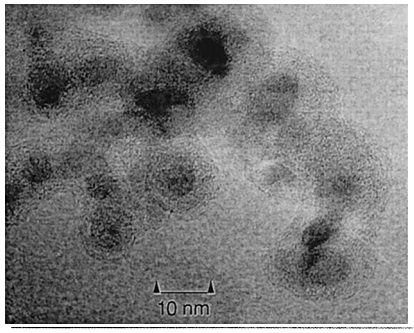

Figure 1a: Transmission electron micrograph of a polymer coated γ-Fe_2O_3 nanopowder. This material consists of 30 Vol-% ceramic and 70 Vol-% polymer.

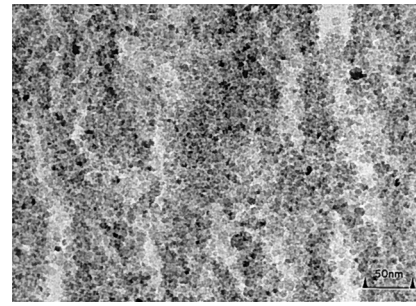

Figure 1b: Transmission electron micrograph from a compacted polymer coated γ-Fe_2O_3 nanopowder. This material consists of 50 Vol-% ceramic and 50 Vol-% polymer. The striations are artefacts caused by sample preparation in an ultramicrotome.

Table 1. Overview of the samples and results of pycnometry and gravimetry.

#	Kernel	Polymer coating	True Density [g/cm^3]	Open Porosity [%]	Polymer Content [Vol-%]
1	n–Al_2O_3	$C_{20}F_{42}$	2,38	20	47
2	n-Al_2O_3	H_2C=CH-$COOCH_2(CF_2)_2CF_3$	2,44	48	46
3	n-Al_2O_3	H_2C=CH-$COOCH_2(CF_2)_2CF_3$	2,28	48	49
4	n-Al_2O_3	H_2C=C(CH_3)-$COOCH_3$	2,35	20	53
5	n-Al_2O_3	H_2C=C(CH_3)-$COOCH_2CH_2NCO$	2,13	29	50
6	n-Al_2O_3	F_3C-$(CF_2)_9CH_2CH_2I$	2,33	16	70
7	n-Al_2O_3	F_3C-$(CF_2)_{10}COOCH_3$	2,27	15	75
8	n-Al_2O_3	H_2C=CH-$COO(CH_2)_2(CF_2)_9CF_3$	2,26	8	70
9	$C_{20}F_{42}$	-	2,18	5	100
10	n-Al_2O_3	-	2,33	55	0

The results of pycnometry and gravimetry in Table 1 show that the lowest porosity (20% and less) is obtained with polymers containing fluorinated-chains as well as acrylic or methacrylic groups. Additionally, a combination with high volume fraction of polymer is of advantage. As n-Al_2O_3 is amorphous, the density is only 65 % of the bulk

density of γ-Al_2O_3. Since the open porosity of the compacted materials varied from 55 to 5%, the values measured for the permittivity were corrected for porosity using Looyenga's theory,[10] not considering percolation effects. Bruggeman's formula[11] lead to similar results. These models are generally in use to evaluate composition dependent properties of isolated spherical particles in a matrix. In contrast, Lichtenegger's logarithmic mixture rule,[12] usually applied for layered materials with the layers either parallel or normal to the applied field did not lead to reasonable results. In the formulae shown in Figure 2, *m* denotes the porosity, *p* the particles and *V* the volume fraction, respectively. Compacted pure n-Al_2O_3 and $C_{20}F_{42}$ were used as reference materials.

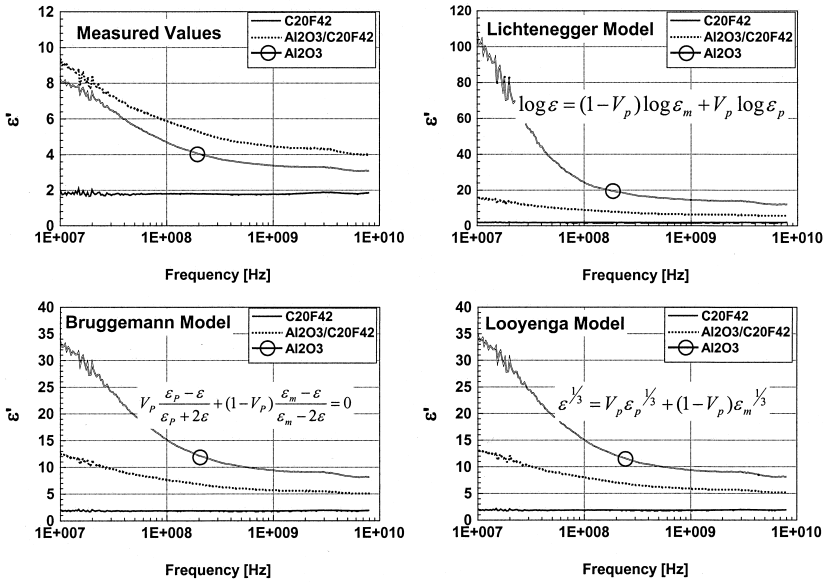

Figure 2. Comparison of three models for porosity correction vs. uncorrected measured values. Details of the specimen are given in Table 1 (#1, #9, #10).

Figure 2 compares the real part of permittivities ε' of a n-Al_2O_3/$C_{20}F_{42}$ nanocomposite and the pure compounds. These Figures show the data "as measured" and after evaluation with the different models for porosity correction. The polymer exhibits no frequency dependency, as it is known for Teflon. The pure n-Al_2O_3 shows strong frequency dependency. The measured values for the composite, not corrected for porosity, are increased as compared to those of pure n-Al_2O_3. This clearly indicates the need of a correction for porosity. Lichtenegger's model results in unreasonably high ε'-values for the ceramic phase, whereas the values for the polymer and the composite

seem to be reasonable. Bruggemann's as well as Looyenga's formulae led to similar results for all three samples. The corrected data show that the frequency dispersion of the composite is reduced, as compared to the pure ceramic phase. The loss of accuracy of the algorithm for the evaluation can be seen since all materials seem to exhibit weak maximum in the range of 4 GHz.

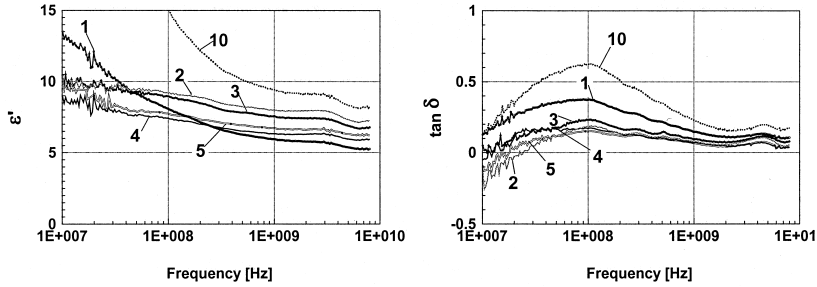

Figure 3. Real part and tan δ of the permittivity for various γ-Al_2O_3/polymer nanocomposites with approximately 50 Vol-% of polymer. The numbers correspond to the sample numbers in Table 1.

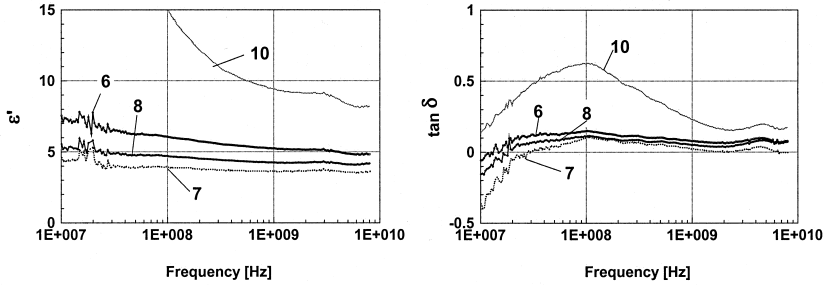

Figure 4. Real part and tan δ of the frequency dispersion behaviour for different fluoropolymers with 70 Vol-% of polymer. The numbers correspond to the sample numbers in Table 1.

Figure 3 clearly shows a decreasing complex permittivity with increasing polymer content of the nanocomposites. Compared to the permittivity of polymers, permittivity and frequency dependencies are increased but remain smaller than these values of the pure ceramic material. Except for $C_{20}F_{42}$ coated particles, the tendency in the behaviour is similar for all polymers used. This material (#1) exhibits the most pronounced frequency dependency, decreasing from the highest value at 10 MHz to the lowest value at 8 GHz.

Figure 4 shows a similar behaviour of the samples containing approximately 70 Vol-% of polymer. With this high polymer content, the frequency dispersion observed is very

small. The various polymers are not showing significant differences in their behaviour. As expected, tan δ of the composites containing 70 Vol-% polymer are lower than tan δ of the material with 50 Vol-% polymer.

Discussion and Conclusions

The high frequency permittivities of ceramic polymer nanocomposites show, after correction for porosity clear trends. Lichtenegger's logarithmic model, traditionally used for layered composite materials, is not applicable to correct the high porosity content of the samples.

Models used for isolated spherical particles in a matrix, not considering percolation, as the models of Bruggeman and Looyenga, lead to most reliable results. The analysed samples show the classical dielectric behaviour of composites: decreasing permittivity with increasing polymer content. Additionally, tan δ decreases with decreasing porosity and increasing polymer content. This behaviour is comparable to conventional ceramic/epoxy composites[13] or to filled polymers.[14] Ceramic/polymer nanocomposite materials can be described as composites with the polymer representing the matrix with separated ceramic inclusions. Composites with $C_{20}F_{42}$ as coating behave different exhibiting a more pronounced frequency dependency. The other polymers, derived from MMA or different fluoropolymers behave similar.

This paper has proven the possibility of combining interesting materials properties of ceramics and polymers in a nanocomposite for producing new, functional materials with altered properties.

[1] D. Vollath, B. Seith, D. V. Szabó, German Patent DE19638601C1, **1998**.
[2] D. Vollath, D. V. Szabó, J. Fuchs, *Nanostruc. Mater.* **1999**, *12*, 433.
[3] D. Vollath, D. V. Szabó, J. Fuchs, *Mat. Res. Soc. Symp. Proc.* **1999**, *577*, 443.
[4] L. Néel, *Comp. Rend.* **1949**, *228*, 664.
[5] D. V. Szabó, D. Vollath, *Adv. Mater.* **1999**, *11*, 1313.
[6] D. Vollath, *KfK-Nachrichten* **1993**, *25*, 139.
[7] A. M. Nicolson, G. F. Ross, *IEEE Trans. Instrum. Meas.* **1970**, IM-19, 377.
[8] Hewlett Packard, Product Note 8510-3.
[9] R. Pelster, private communication, **2000**.
[10] H. Looyenga, *Physica* **1965**, *31*, 401.
[11] D. A. G. Bruggmeman, *Ann. Phys.* **1935**, *24*, 636.
[12] K. Lichtenegger, *Phys. Z.* **1908**, *10*, 1005.
[13] H. D. Choi, H. W. Shim, K. Y. Cho, H. J. Lee, C. S. Park, H. G. Yoon, *J. Appl. Polym. Sci.* **1999**, *72*, 75.
[14] C. Brosseau, P. Quéffélec, P. Talbot, *J. Appl. Phys.* **2001**, *89*, 4532.